ISTITUTO NAZIONALE DI FISICA NUCLEARE - ISTITUTO NAZIONALE DI FISICA NUCLEARE - ISTITUTO NAZIONALE DI FISICA NUCLEARE - ISTITUTO NAZIONALE DI FISICA NUCLEARE - ISTITUTO NAZIONALE DI FISICA NUCLEARE - ISTITUTO NAZIONALE DI FISICA NUCLEARE - ISTITUTO NAZIONALE DI

Laboratori Nazionali di Frascati

LNF-89/007R)
14 Febbraio 1989

C. Sanelli:

LISA UNDULATOR PROJECT

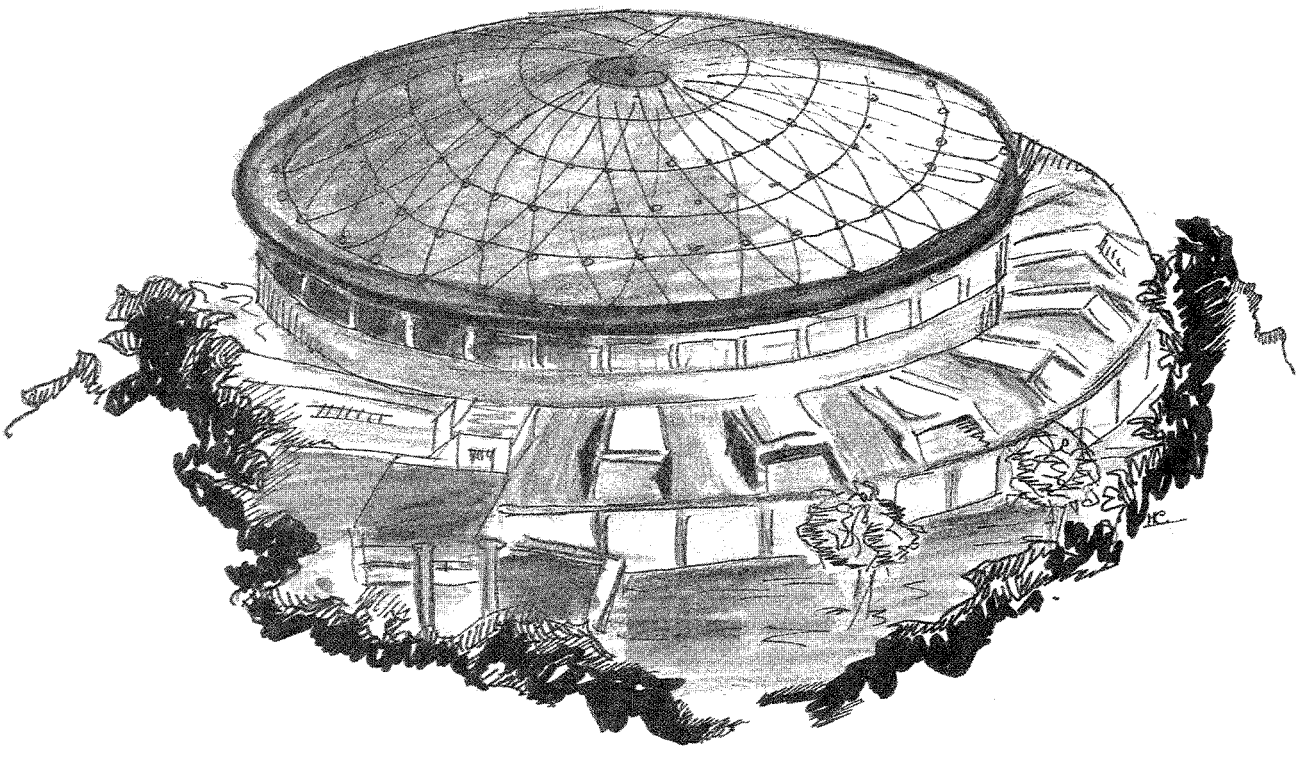

Servizio Documentazione
dei Laboratori Nazionali di Frascati
P.O. Box, 13 - 00044 Frascati (Italy)

INFN - Laboratori Nazionali di Frascati
Servizio Documentazione

LNF-89/007(R)
14 Febbraio 1989

LISA UNDULATOR PROJECT

C. Sanelli
INFN - Laboratori Nazionali di Frascati, P.O.Box 13, 00044 Frascati (Italy)

ABSTRACT

The superconducting accelerator LISA is under construction. The 25 MeV electron beam will be utilized for a Free Electron Laser experiment having the first harmonic in the infrared region. The design of the undulator to be used for the experiment and the status of the construction of a prototype with only seven plus two half poles is reported.

1. - INTRODUCTION

The linear accelerator LISA[1], a test superconducting electron linac, is under construction at LNF. This machine, integral part of the research and development program in the field of RF superconductivity, is aimed at studying some of the problems of SC linacs and its specifications are tailored to the requirements of an infrared Free Electron Laser (FEL).

The main parameters of LISA are given in Table I.

Table I - Main parameters of the LISA accelerator.

Energy	$25 \div 49$	MeV
Bunch length	2.5	mm
Peak current	5	A
Duty cycle	≤ 2 %	
Average macropulse current	2	mA
Energy spread (@25 MeV)	$2*10^{-3}$	
Micro bunch rep. frequency	50	MHz
Invariant emittance	10^{-5}	π m rad

The characteristic of the beam of the SC linac well match the requirements for a high efficiency Free Electron Laser in the infrared region using an undulator of 5 cm period and field parameter $0.5 \leq k \leq 1.5$; doubling the beam energy and working on the 3rd harmonic emission line it will be also possible to reach the visible region [2].

The main parameters of the FEL are given in Table II.

As reported elsewhere[3] the undulator can be a standard electromagnetic device or a hybrid one; in this note the design and the status of construction of the prototype of the electromagnetic undulator are presented.

Table II - Main parameters of the Free Electron Laser experiment.

Beam energy	25	MeV
Number of undulator periods	≤50	
Undulator wavelength	5	cm
Radiation wavelength	12÷22	μm
Optical cavity length	6	m
Cavity passive losses	2 %	

2.- ELECTROMAGNETIC DESIGN

Some parameters as the energy , 25 MeV, the period of the undulator period, 5 cm, and the maximum value of K=1.5 have been set ; the peak magnetic field can be calculated from :

$$K=93.4 * B_{[T]} * \lambda q_{[m]}; \qquad (1)$$

where B is the peak field and λq is the undulator period; one obtain the requested value of 0.32[T]. For the electromagnetic design another parameter has needed: the gap between the poles that has been chosen to be 2 cm.

The ratio between the length of the pole and the length of the window, where the coils have to be mounted, is the same of Lela undulator[4]; a length of the pole of 12.5 mm, and a length of the window of the same value were chosen. A first calculation was made [3] using the two dimensional codes MAGNET and POISSON; with a current of 4000 Amp-turns applied for pole, to which the maximum iron saturation is about 2.1 [T], a peak field of 0.34 [T] was obtained from Magnet and 0.33 [T] from Poisson code.

A more accurate calculation has been made with the three dimensional code MAGNUS, with which two different configurations have been studied: the central pole and the end pole. In the last one the configuration with four terminal poles without and with clamping plate has been investigated.

2.1. - Central pole

The central pole will have a transversal dimension of 15 cm and the thickness of the return yoke will be 3 cm.

Fig. 1 shows the half central pole evidencing the mesh generated by the pre processor KUBIK. The air surrounding the pole is not shown in figure. Using the symmetries and particularly the surfaces where the Dirichlet conditions are satisfied and the field is perpendicular to the surface, the analysis can be restricted to 1/4 of the pole geometry : Figure 1 shows the half right upper pole.

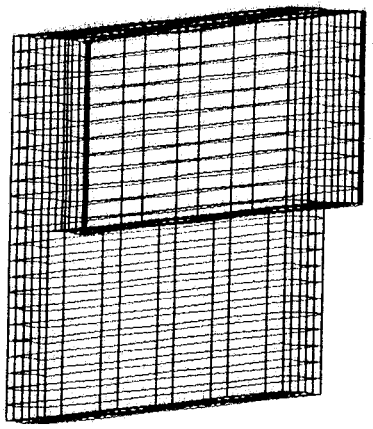

FIG. 1 - Half upper central pole: mesh generated by KUBIK.

Fig. 2 shows the coils as "seen by the code". Differently from other codes, Magnus can accept infinite, semi-infinite and finite straight bars, prismatic solid conductors, infinite, semi-infinite and finite straight filaments, flat strips, full circular and circular arc filaments, circular coils and circular arcs of rectangular cross-section. In this case the coil has been constructed with two straight bars of rectangular cross section (25 * 5 mm^2), and two 180° arcs, which are the heads of the coil, having the same cross section. The upper and lower coils must be specified for a correct solution in the domain where the solution has to be found; this is possible because the mesh generation is independent from the excitation currents that must be specified only when running Magnus, the Maxwell's equation solver.

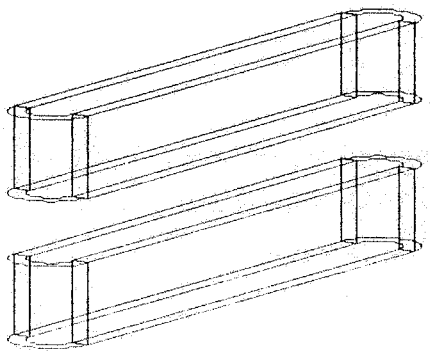

FIG. 2 - The excitation coils.

Fig. 3 shows the vertical component of the magnetic field along the beam direction. This curve is very similar to a cosinusoid and the peak field is predicted to be 0.365 [T]. If this value will be reached, a K of 1.7 can be obtained with a first harmonic wavelength :

$$\lambda = \lambda q * (1 + K^2/2)/ (2 * \gamma^2) = 25 \ [\mu m]; \qquad (2)$$

where $\gamma = E/Eo$, being E the beam energy (25 MeV) and Eo the rest energy of the electron (0.51 MeV). The curve in Fig.3 is not a perfect cosinusoid, but the values calculated by Magnus are a little greater than a perfect cosinusoid. The difference is shown in Fig. 4, where a cosinusoid is overlapped on Magnus curve. To evaluate this difference, the field integral along the beam axis has been evaluated; the integral of the curve calculated with the code is 2.968 [T*mm] instead of 2.902 [T*mm] for the perfect cosinusoid; the difference between them is about 2 % and is concentrated in the central zone of the curve.

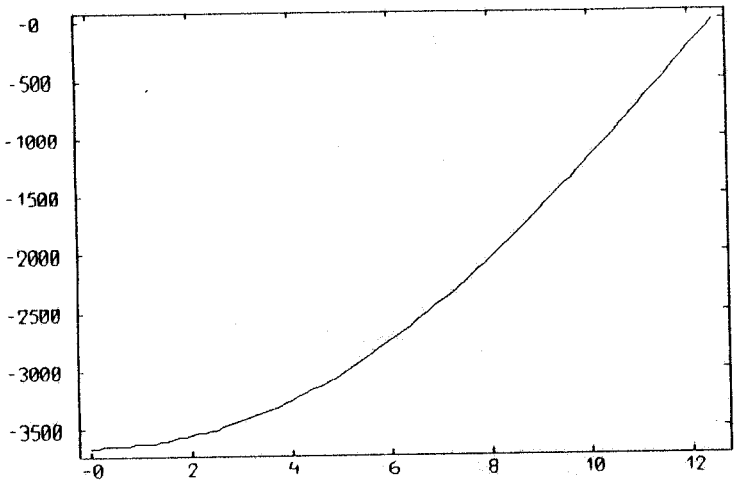

FIG. 3 - Vertical component of B[Gauss] along beam axis (mm).

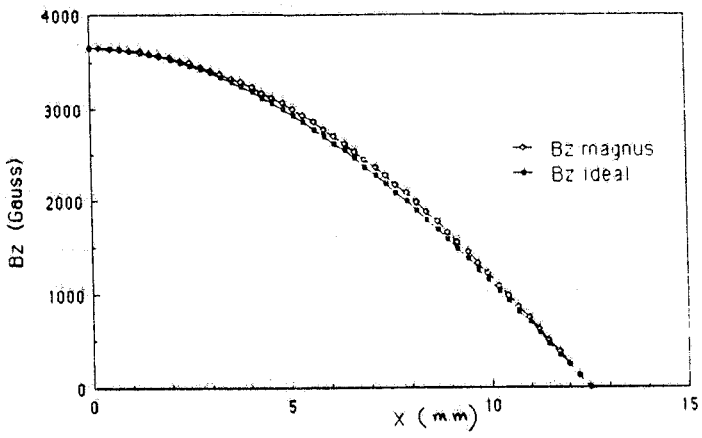

FIG. 4 - The Magnus field compared to an ideal cosinuosoid.

In our case, the ratio between the maximum vertical field at the gap center Bo, and the corresponding field at the pole surface, Bp, is 0.717 instead of 0.799 of the Lela undulator case, according to the Pool and Walker curve[5], which gives this ratio as a function of the ratio between the undulator period λq and the gap height, h :

$$Bo/Bp=[1- \sinh (x) / (3 * \sinh(3x)]/\{[1 - \tanh(x) / (3 * \tanh(3x))] * \cosh(x)\} \qquad (3)$$

where $x = \pi / (\lambda q / h)$.

Fig. 5 shows the two operating points on the curve.

The value of the field at the pole surface is confirmed by the code. Fig. 6 shows the vertical component of B along the vertical axis and a value of 0.477 [T] is found at the center of the pole; the maximum saturation value in the iron is about 2.13 [T].

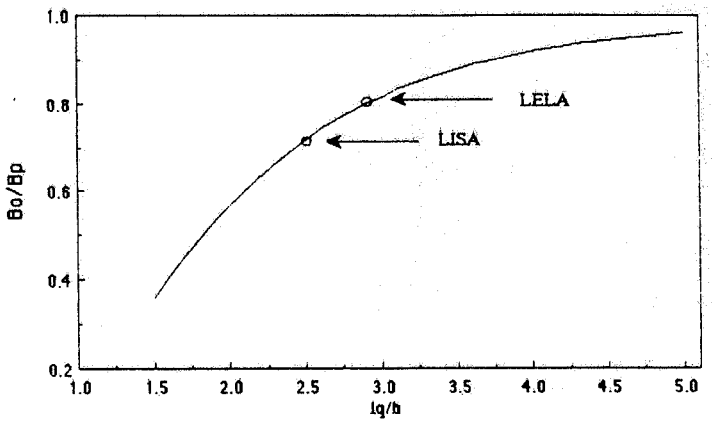

FIG. 5 - LISA and LELA undulator working points.

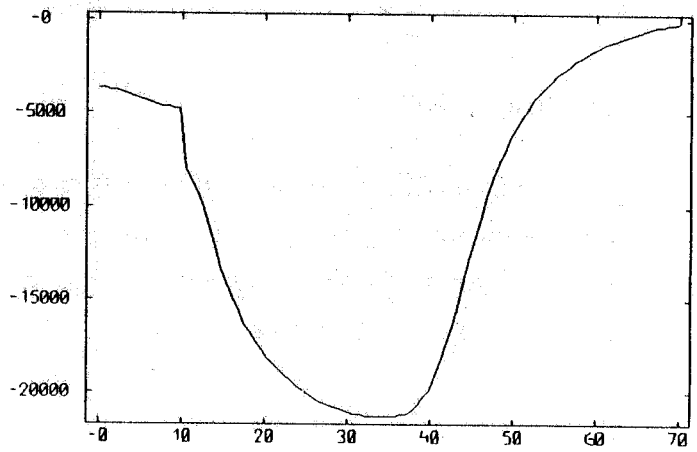

FIG. 6 - B[Gauss] vertical component along the vertical axis at the pole center.

If one approximates the field off the midplane as follows :

$$Bz(x,z) = Bo * \cos(2\pi x / \lambda q) * f(z); \quad (4)$$

where x is the beam direction and z the vertical direction, the function f(z) assumes the following expression, for $0.0 \leq z \leq 5$ mm:

$$f(z) = 1 + b z^2; \quad (5)$$

with $b = 6.6 * 10^{-3}$ mm^{-2}.

The field in the radial direction, y axis, is quasi-constant. For $y \geq \pm 61$ mm there is a variation less than 1%, which can be described by the quadratic term of Tailor expansion in the form :

$$B(y) \approx Bo + (0.5 * \partial B^2/\partial y^2) * y^2. \quad (6)$$

In the range -30≤ y ≤+30 mm, the term $\partial B^2/\partial y^2$ is equal to -1.27 * 10^{-2} [Gauss/mm^2]. This term gives the value of the sextupole introduced by the undulator.

Fig. 7 shows a general view of the half upper pole with a quarter of the coil and some flux lines from the yoke, passing through the pole and going down to the inner pole. Other lines, coming from the yoke, exit from the lateral surface of the pole and go toward the near pole. This is due to the lateral reluctance which is comparable to the reluctance between upper and lower pole.

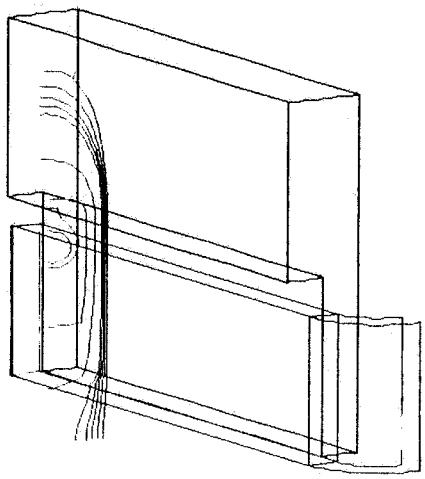

FIG. 7 - Half upper pole: pole profile, coil and flux lines.

2.2.- End pole

The geometry shown in Fig. 8 has been generated using the maximum number of mesh points of the code. In this picture the four end poles are visible. In particular the first pole on the left is only half pole because of the symmetry conditions. Since a mirror-like condition this pole can be considered as a full pole.

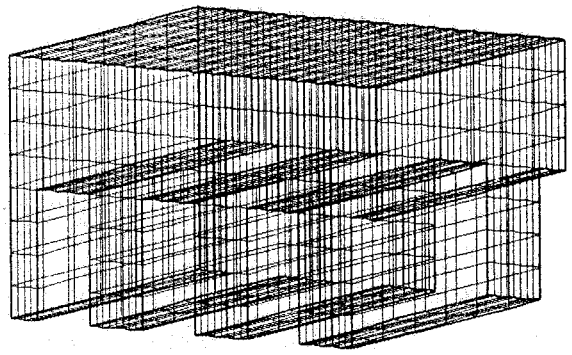

FIG. 8 - Four upper end poles: mesh generated by KUBIK.

The applied Amper-turns in the first three poles are 4000, while in the end pole 2000 A-turns are applied in a first run and then gradually decreased to 1575 A-turns, for reaching a zero vertical field component integral. During this attempt, one can observe that the variation of the current in the end pole causes the peak field of the full poles to change in the same direction of the variation of the end pole.

Fig. 9 shows the vertical component of the field along the electron beam direction.

The peak field is not equal of the three full poles and even the zero-crossing point is shifted outwards, with a slow decreasing of the field towards the zero. The peak fields

predicted by the code are respectively from left side, in Tesla : -0.358, 0.375, -0.377, 0.188 [T].

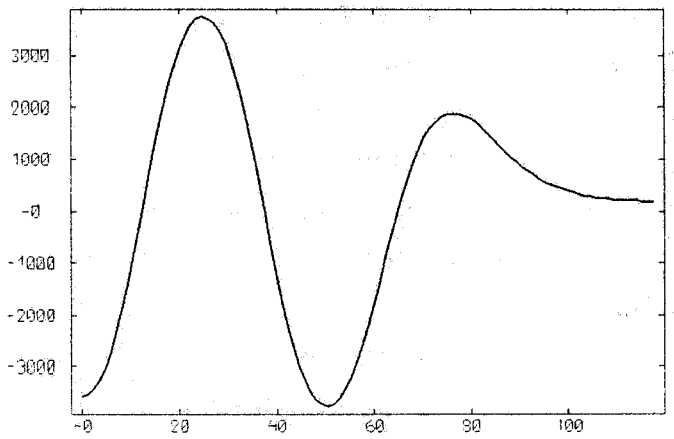

FIG. 9 - Vertical B[Gauss] component along beam axis (mm) for geometry in Fig. 8.

To obtain a more accurate field distribution a shield has been applied at the end of the undulator, allowing a free space of 20 mm in vertical and 150 mm in horizontal. The thickness of the shield has been chosen 12.5 mm.

Fig. 10 shows the new iron geometry and Fig. 11 reports the Bz component as a function of the x direction.

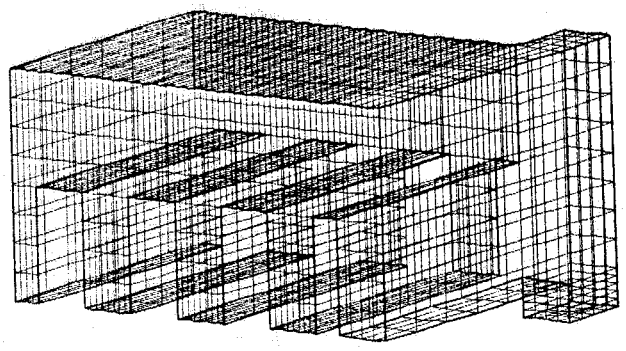

FIG. 10 - Four upper end poles with shield: mesh generated by KUBIK.

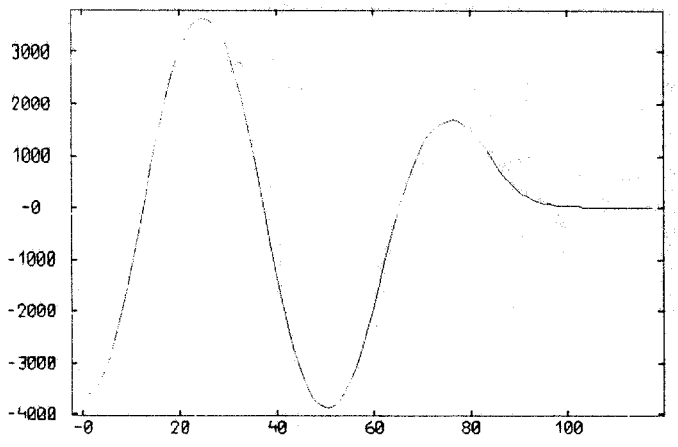

FIG. 11 - Vertical B[Gauss] component along beam axis (mm) for geometry in Fig. 10.

The shield determines a strong change in the peak field values, the first peak changing from -0.358 to -0.367 [T], the second from 0.375 to 0.366 [T], the third from -0.368 to -0.388. The peak field of the half pole decreases from 0.188 to 0.168 [T]. The shield compresses the flux towards the central zone of the undulator increasing the negative peaks and decreasing the positive ones.

The values of the field beyond the shield is now reduced, at x=117.5 mm, to about 9 Gauss instead of 190 Gauss of the previous situation. Since it is a small value, the integral of the vertical component of the field has been calculated from x=0.0 to x=118.5 mm, obtaining -10.7 Gauss *m.

Fig. 12 shows the Bz component along the beam direction 5 mm off the symmetry plane.

Fig. 13 shows some field flux lines in the last generated structure.

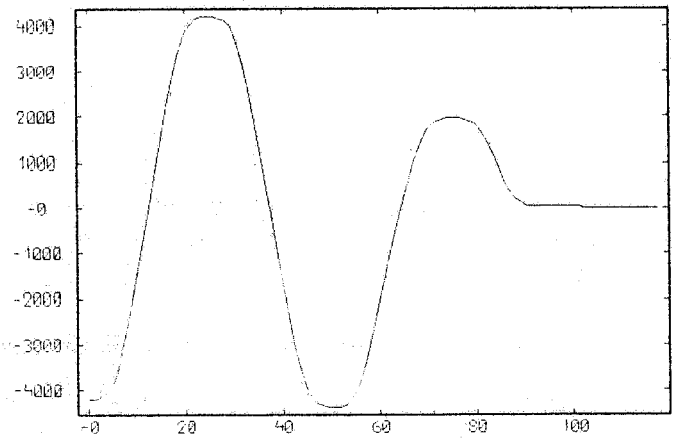

FIG. 12 - Vertical B[Gauss] component along beam axis (mm), 5 mm off the symmetry plane.

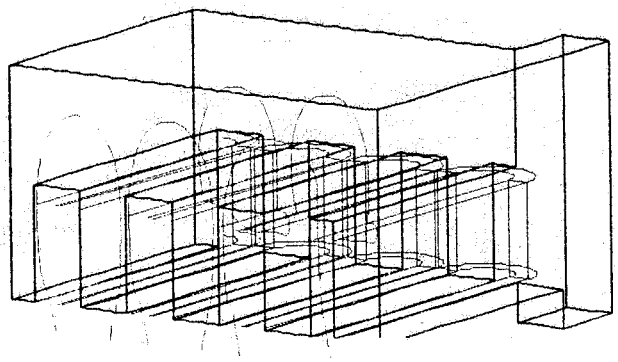

FIG. 13 - Field lines and coils in the structure of Fig. 10.

By means of Poisson code the magnetic field with respect the current is drawn and reported in Fig. 14. The maximum value of the current is 4000 A, even though the curve is extrapolated to 6000 A.

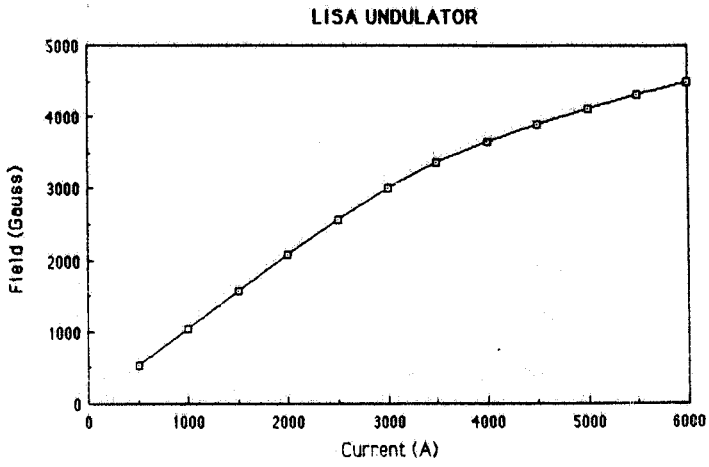

FIG. 14 - Field versus current (POISSON code).

Some considerations have been also done about the mechanical forces, using the Poisson code. Fig. 15 shows the attractive force between the poles and the force acting on the coil due to the horizontal magnetic field in which the coil is immersed because of the flux between two contiguous poles. The two forces have about the same value for any operating point. This situation is confirmed by the three dimensional code that, in the

region composed by the full pole and its coil, gives a total attractive force of just 1.6 kg. Fig. 16 shows the Hoop force acting on the coil per meter of length ; at the maximum field value this force is about 15 kg per meter.

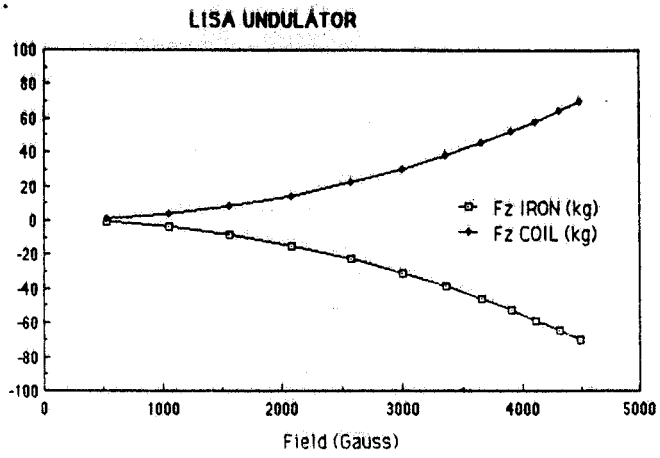

FIG. 15 - Vertical forces between poles and acting on the coil (POISSON code).

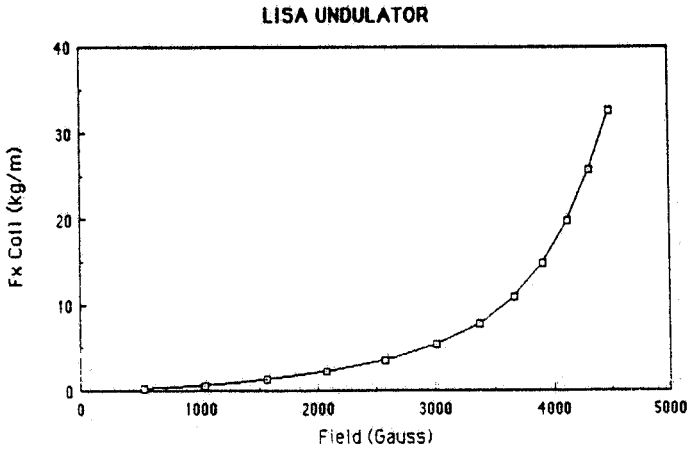

FIG. 16 - Hoop force on the coil (POISSON code).

3.- COIL DESIGN

To obtain 4000 Amperturns, a 5 turn coil has been proposed. The size of the standard conductor (5 * 5 mm^2, with 3 mm hole) was too large to be mount in a 6.25 mm window. Therefore a special Copper conductor having a square section of 4.5 * 4.5 mm^2 has been manufactured. At the moment an Italian factory is winding 20 coils for the undulator prototype.

Table III reports the main parameters of the electromagnet.

4. - THE PROTOTYPE

To check the validity of the magnetic calculation a prototype is now under construction. This prototype is composed of 9 couples of poles. The 7 central couples will be electrically powered in series while the end couples will be independently powered in order to obtain the field integral to vanish. The iron is under processing; each half magnet

will be obtained from an ARMCO iron block and the poles will be processed by an electronically-controlled milling machine.

Table III - Main parameter list of the electromagnet undulator.

Energy	25	MeV
Maximum field on axis	0.36	T
Period	0.05	m
Deflection parameter K	1.7	
Pole length	0.0125	m
Pole height	0.03	m
Pole width	0.15	m
Yoke thickness	0.03	m
Pole length/window ratio	1	
Gap	20	mm
Amperturns per pole	4000	
Current	800	A
Current density	60.7	A/mm^2
Turns per coil	5	
Copper conductor	4.5 * 4.5 Ø 3	mm^2
Coil resistance	≈3.05 mΩ	(at 60°C)
Power per coil	≈ 2	kW
Voltage per coil	≈ 2.4	V
Inductance per coil	≈ 3	μH

Figures 17, 18, 19, 20, show the mechanical drawings of the undulator and respectively the electrical and hydraulic connection side, the front view, the plan of the central cross section and an assembling view.

The mechanical design has been completely developed by the CAD-CAE Engineering Group of the Technical Division.

The Mechanical Group of the Accelerator Division is involved in the construction of the prototype and in the definition of the cooling system parameters.

The prototype will be tested by mapping the field with an Hall probe coordinatometer system. If the expected field value will be reached, the prototype will be used as central module of the final undulator. To have full flexibility, nine modules, of five periods each, will be realized obtaining a total of 97 couples of full pole plus 2 couples of end poles, for a total of 49 periods and a total mechanical length of 2.475 [m].

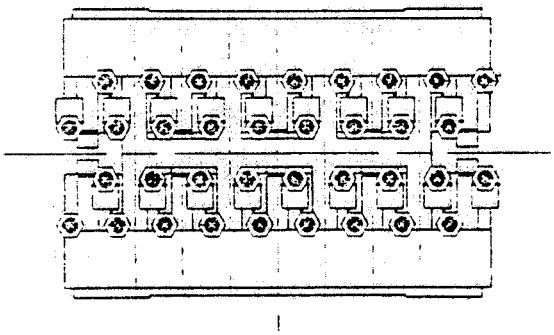

FIG. 17 - Undulator Prototype: electrical and hydraulic connection side.

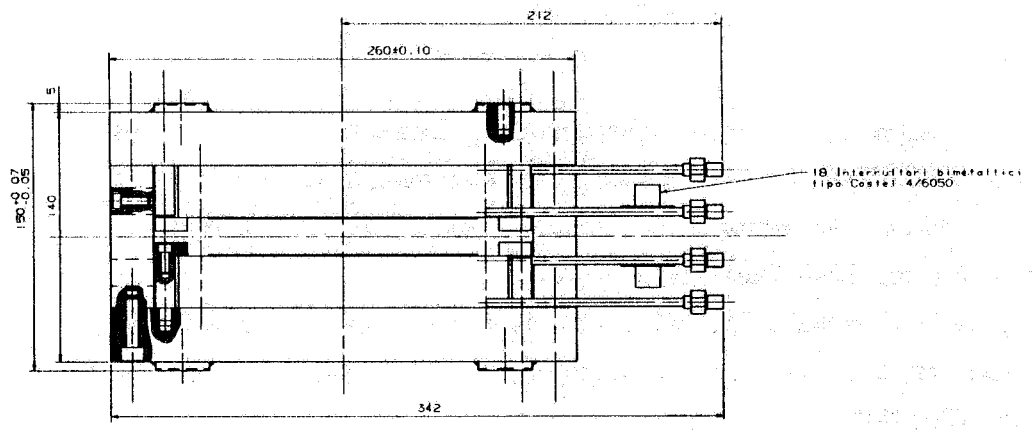

FIG. 18 - Undulator Prototype: front view.

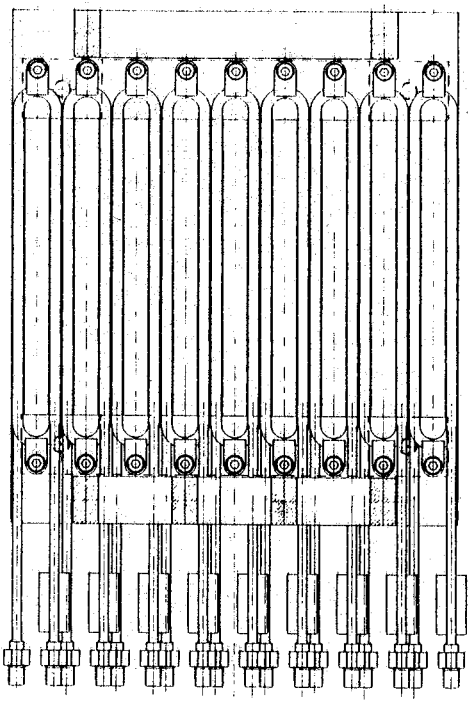

FIG. 19 - Undulator Prototype: plan of the central cross section.

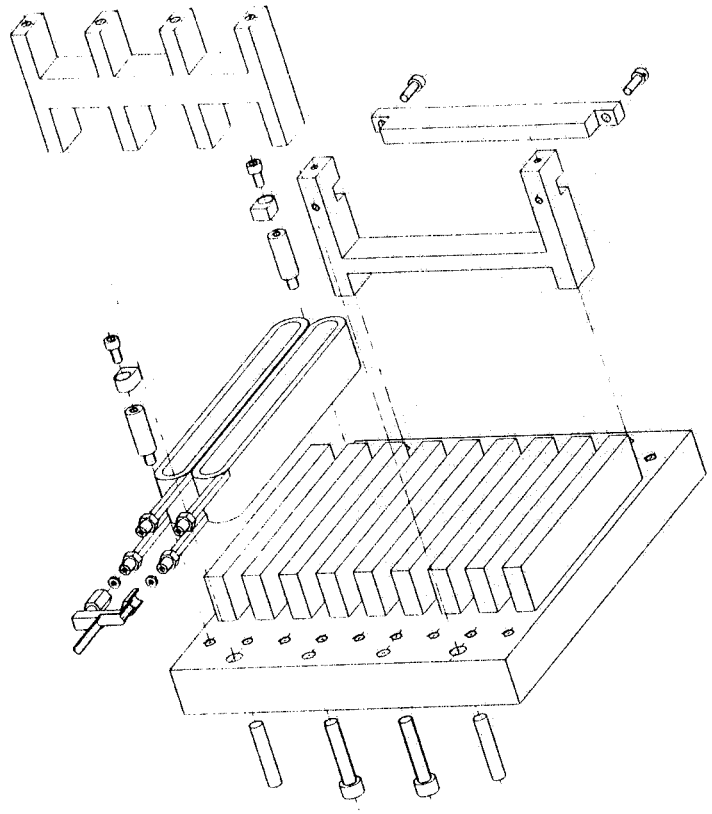

FIG. 20 - Undulator Prototype: assembling view.

References

[1] A. Aragona et al.:"Work on superconducting linacs in progress in Frascati", Proc. Linac '88 CEBAF, 2-7/10, Williamsburg, Virginia U.S.A.(1988).

[2] M. Castellano:"An infrared free electron laser on the superconducting linac Lisa" Internal report LNF-88/04 (R), (1988).

[3] A. Cattoni, C. Sanelli: "Metodi di calcolo di ondulatori in vista della costruzione di un modello di Linac s.c. con un esperimento di Free Electron Laser" Report LNF-87/14 (R) (1987).

[4] R. Barbini et al.: "The lela undulator" Nuclear Instr. & Meth. 190 (1981) 159-166

[5] M.W. Poole and R.P.Walker, Daresbury Report DL/SCI/P215A (1980)